

Elsevier Editorial System(tm) for Quaternary International  
Manuscript Draft

Manuscript Number: QUATINT-D-12-00191R1

Title: Multiproxy evidence for abrupt climate change impacts on terrestrial and freshwater ecosystems in the Ol'khon region of Lake Baikal, central Asia

Article Type: Baikal-Hokkaido

Keywords: climate reconstruction; pollen; ostracod; geochemistry; shallow lake, central Asia

Corresponding Author: Dr Anson W. Mackay, Ph.D.

Corresponding Author's Institution: UCL

First Author: Anson Mackay

Order of Authors: Anson Mackay; Elena Bezrukova; John Boyle; Jonathan Holmes; Virginia Panizzo; Natalia Piotrowska; Alexander Shchetnikov; Ewan Shilland; Pavel Tarasov; Dustin White

Manuscript Region of Origin: RUSSIAN FEDERATION

Abstract: A palaeolimnological study of Lake Khall was undertaken to reconstruct impacts from five thousand years of climate change and human activity in the Ol'khon region of Lake Baikal. Taiga biome dominated regional landscapes, although significant compositional turnover occurred due to the expansion of eurythermic and drought resistant Scots pine. Climate during the mid-Holocene was wetter than the present, and Lake Khall was fresh, with abundant molluscs. By 4.4 cal ka BP, sedimentary geochemistry indicated a gradual change in lake water chemistry with an increase in lake salinity up to the present day, most likely controlled by groundwater influences. Vegetation turnover rate was highest between 2.75 - 2.48 cal ka BP, with the onset of drier, more continental climate, which resulted in an influx of aeolian particles to the lake. This abrupt shift was coincident with ice rafted debris event (IRD-2) in North Atlantic sediments and an attenuation of the East Asian summer monsoon. A second arid period occurred shortly afterwards (2.12 - 1.87 cal ka BP) which resulted in the decline in ostracod numbers, especially *Candona* sp. A rather more quiescent, warmer period followed, between 1.9 - 0.7 cal ka BP, with very little change in vegetation composition, and low amounts of detrital transfer from catchment to the lake. Peak reconstructed temperatures (and low amounts of annual precipitation) were concurrent with the Medieval Climate Anomaly. Between 0.77 - 0.45 cal ka BP, climate in the Ol'khon region became colder and wetter, although Lake Khall did not become more fresh. Cold, wet conditions are seen at other sites around Lake Baikal, and therefore represent a regional response to the period concurrent with the Little Ice Age and IRD-0. After AD 1845 the region warms, and *Pediastrum* appears in the lake in high abundances for the first time. We ascribe this increase to nutrient enrichment in the lake, linked to the rapid increase in regional pastoral farming.

1 Multiproxy evidence for abrupt climate change impacts on terrestrial and freshwater  
2 ecosystems in the Ol'khon region of Lake Baikal, central Asia.

3

4 Anson W. Mackay<sup>a,\*</sup>, Elena V. Bezrukova<sup>b</sup>, John F. Boyle<sup>c</sup>, Jonathan A. Holmes<sup>a</sup>, Virginia N.  
5 Panizzo<sup>a</sup>, Natalia Piotrowska<sup>d</sup>, Alexander Shchetnikov<sup>e</sup>, Ewan M. Shilland<sup>a</sup>, Pavel Tarasov<sup>f</sup>,  
6 Dustin White<sup>g</sup>

7

8 \* Corresponding author: *Email address:* [a.mackay@ucl.ac.uk](mailto:a.mackay@ucl.ac.uk)

9 Phone : +44 (0)20 7679 0558 ; Fax : +44 (0)20 7679 0565

10

11 <sup>a</sup>*Environmental Change Research Centre, Department of Geography, UCL, Gower Street,*  
12 *London, WC1E 6BT, UK.*

13 Email: [a.mackay@ucl.ac.uk](mailto:a.mackay@ucl.ac.uk)

14

15 <sup>b</sup>*Institute of Geochemistry, Russian Academy of Sciences, Siberian Branch, Irkutsk, Russia.*

16 Email: bezrukova@igc.irk.ru

17

18 <sup>c</sup>*Department of Geography, The University of Liverpool, Roxby Building, Liverpool L69 7ZT,*  
19 *UK.*

20 Email: jfb@liverpool.ac.uk

21

22 <sup>d</sup>*Institute of Physics, Department of Radioisotopes, GADAM Centre of Excellence, Silesian*  
23 *University of Technology, Krzywoustego 2, 44-100 Gliwice, Poland.*

24 Email: natalia.piotrowska@polsl.pl

25

26 <sup>e</sup>*Institute of Earth's Crust, Russian Academy of Sciences, Siberian Branch, Irkutsk, Russia.*

27 Email: shchet@crust.irk.ru

28

29 <sup>f</sup>*Institute of Geological Sciences, Palaeontology, Freie University Berlin, Malteserstrasse 74-*  
30 *100, Building D, 12249 Berlin, Germany.*

31 Email: ptarasov@zedat.fu-berlin.de

32

33 <sup>g</sup>*Archaeology, University of Southampton, Avenue Campus, Southampton, SO17 1BF, UK.*

34 Email: dustin.white@soton.ac.uk

35

36

37

38

39 **Abstract**

40

41 A palaeolimnological study of Lake Khall was undertaken to reconstruct impacts from five  
42 thousand years of climate change and human activity in the Ol'khon region of Lake Baikal.  
43 Taiga biome dominated regional landscapes, although significant compositional turnover  
44 occurred due to the expansion of eurythermic and drought resistant Scots pine. Climate during  
45 the mid-Holocene was wetter than the present, and Lake Khall was fresh, with abundant  
46 molluscs. By 4.4 cal ka BP, sedimentary geochemistry indicated a gradual change in lake  
47 water chemistry with an increase in lake salinity up to the present day, most likely controlled  
48 by groundwater influences. Vegetation turnover rate was highest between 2.75 – 2.48 cal ka  
49 BP, with the onset of drier, more continental climate, which resulted in an influx of aeolian  
50 particles to the lake. This abrupt shift was coincident with ice rafted debris event (IRD-2) in  
51 North Atlantic sediments and an attenuation of the East Asian summer monsoon. A second  
52 arid period occurred shortly afterwards (2.12 – 1.87 cal ka BP) which resulted in the decline  
53 in ostracod numbers, especially *Candona* sp. A rather more quiescent, warmer period  
54 followed, between 1.9 – 0.7 cal ka BP, with very little change in vegetation composition, and  
55 low amounts of detrital transfer from catchment to the lake. Peak reconstructed temperatures  
56 (and low amounts of annual precipitation) were concurrent with the Medieval Climate  
57 Anomaly. Between 0.77 – 0.45 cal ka BP, climate in the Ol'khon region became colder and  
58 wetter, although Lake Khall did not become more fresh. Cold, wet conditions are seen at  
59 other sites around Lake Baikal, and therefore represent a regional response to the period  
60 concurrent with the Little Ice Age and IRD-0. After AD 1845 the region warms, and  
61 *Pediastrum* appears in the lake in high abundances for the first time. We ascribe this increase  
62 to nutrient enrichment in the lake, linked to the rapid increase in regional pastoral farming.

63

64

65

66

67

68 **Keywords:** climate reconstruction; pollen; ostracod; geochemistry; shallow lake, central Asia

69 **1. Introduction**

70

71 Since 2001 a major interdisciplinary programme (Baikal Archaeology Project) has sought  
72 to characterise Holocene cultural dynamics among hunter-gatherer and pastoralist populations  
73 in central Asia (Weber et al., 2010). Results from this on-going research have redefined our  
74 understanding of hunter-gatherer adaptive strategies during the Neolithic–Bronze Age,  
75 including aspects of culture, subsistence and diet, mobility patterns, genetic structure, and  
76 social and political relations. Most of these new archaeological data have been derived from  
77 numerous well-preserved formal cemetery contexts, which has allowed detailed analyses of  
78 human skeletal remains. Focus has especially centred on a distinct biocultural discontinuity  
79 during the late Neolithic – early Bronze Age (Weber et al., 2002), and more recently the  
80 expansion of pastoralist populations (Nomokonova et al., 2010).

81 One of the oldest records of human occupation in this region (ca. 9 ka BP) was recorded at  
82 the Sagan-Zaba cove, in the Ol'khon region (known as *Priol'khon'e* in the Russian  
83 geographical literature) of Lake Baikal (Nomokonova et al., in review). The white marble  
84 cliffs adjacent to the cove are world renown for their petroglyphs, dating as far back as 4 ka  
85 BP. Since the late Holocene, pastoralists dominated the Ol'khon region, herding a range of  
86 animals including cattle, sheep, goats and horses (Nomokonova et al., 2010). Subsistence  
87 patterns at Sagan-Zaba were more diverse than neighbouring regions, possibly because of the  
88 relatively harsh environment, such that, unusual for pastoralists, these populations also hunted  
89 *nerpa*, Lake Baikal's freshwater seal.

90 Despite the long history of prehistoric populations around Lake Baikal, there is very little  
91 evidence to suggest that they had a significant impact on regional landscapes (Tarasov et al.  
92 2007). However, the pollen source area of Lake Baikal is vast and indicative of very broad  
93 regional-scale variability (Sugita 1994), such as biomes (Seppä and Bennett, 2003; Tarasov et  
94 al., 2007). One would not necessarily expect therefore Lake Baikal sediments to record  
95 impacts from regional prehistoric populations. Smaller lakes have smaller source areas  
96 (Jacobson and Bradshaw, 1981), and therefore potentially offer a better possibility for  
97 disentangling natural (e.g. climatic) from anthropogenic impacts. Around Lake Baikal,  
98 smaller lakes are increasingly being investigated (e.g. Tarasov et al., 2009; Ptitsyn et al.,  
99 2010; Mackay et al., 2012), although very few studies have looked at palaeoenvironmental  
100 changes in the semi-arid region to the west of the lake (Sklyarov et al., 2010).

101 The principal aim of this study is to provide a detailed palaeolimnological record of  
102 environmental change in the climatically sensitive Ol'khon region of Lake Baikal, where  
103 there is a long, dynamic history of human occupation.

104

105 **2. Geology and regional climate**

106

107 The study area lies to the south of Ol'khon Island on the west coast of Lake Baikal  
108 and is represented by Paleozoic Ol'khon metamorphic terrane (Sklyarova et al., 2002). The  
109 flat-topped Ol'khon Island and Ol'khon region form part of the Middle Baikal inter-basinal  
110 link. Small grabens and horsts shape the link's surface and form linear en-echelon systems.  
111 The grabens are confined to two types of recent faults in the process: northeast linear faults  
112 inherited from the Early Paleozoic structures and north-northeast pull-apart structures related  
113 to late left-lateral strike-slip dislocations of the Baikal rift formation. Numerous fresh and  
114 salt-water lakes are associated with these faults (Sklyarova et al., 2002), with their long-term  
115 existence being dependent on faults draining deep, groundwater horizons (Sklyarov et al.,  
116 2010). The study site, Lake Khall, is located on marble and surrounded by two intrusions –  
117 Birkhinsky in the north (gabbro, gabbro-norites, olivine gabbro) and Tsagan-Zabinsky in the  
118 south (andesites, andesite-basalts and basalts). It is a shallow, isometric, freshwater  
119 bicarbonate lake located in a structural low of one these northeast linear faults. Lake Khall is  
120 probably fed from subaqueous groundwater, and so its chemical composition reflects the  
121 chemistry of the feeder groundwater (Sklyarova et al., 2002). The region is arid to semi-arid  
122 because it sits in the rain shadow of the neighbouring Primorsky Mountain Range (Fig. 1).  
123 Annual precipitation is low between 200 – 350 mm/yr (Atlas Baikala, 1993). Vegetation is

124 therefore a mixture between light coniferous taiga forest with fragmented steppe landscape,  
125 including the Tazheran steppes (Sklyarov et al., 2010).

### 127 3. Methods

128  
129 Fieldwork took place on 26<sup>th</sup> July 2006. pH and conductivity were measured *in situ*  
130 using a Fisher Scientific accumet AP85 pH/conductivity meter. The pH of the surface water  
131 was 9.0 pH units, and conductivity was 790  $\mu\text{S}/\text{cm}$ . Due to time constraints, it was not  
132 possible to conduct a detailed bathymetry of the lake, although a Plastimo Echotest II  
133 handheld depth sounder was used to estimate the deepest region at 3.10 m, from where coring  
134 was undertaken. A 71 mm diameter Livingstone core was initially extracted (44 cm length),  
135 which maintained the surface sediment – water interface, followed by a second overlapping  
136 Livingstone drive of 91 cm. Core location co-ordinates were 106°25'50.70"E, 52°41'14.54"N.

#### 138 3.1 Chronology

139  
140 Extracted lake sediments were highly humified and from many levels it was not  
141 possible to obtain sizeable plant macrofossils for radiocarbon analyses. Radiocarbon dating of  
142 humified sediments was instead performed on total organic carbon (TOC) from 5 bulk  
143 sediment samples. *Potamogeton* seeds were isolated from a further four levels. All nine  
144 samples were radiocarbon dated using accelerator mass spectrometry (AMS) at the Poznan  
145 Radiocarbon Laboratory, Poland (Goslar *et al.*, 2004) (Table 1). The amount of radiocarbon  
146 reservoir effect (i.e. shift towards older ages) was estimated on the basis of <sup>14</sup>C dating  
147 contemporary leaf sample of *Potamogeton* from the littoral region of Lake Khall. The result  
148 of 105.58±0.33 pMC suggests a reservoir age of 100-200 years (Table 1). We have therefore  
149 added the reservoir correction of 150±50 years to the age model for Lake Khall sediment  
150 core.

151 Calibration of radiocarbon dates was undertaken using the Intcal09 calibration curve  
152 (Reimer *et al.*, 2009). The calibration was performed by “Bacon” software simultaneously to  
153 building the calendar age scale for the whole core. In order to produce the age-depth model  
154 this programme simulates the accumulation of deposit through small random increments, and  
155 also takes into account the limitations on accumulation rate and its variability (Blaauw and  
156 Christen, 2011). Although some of the obtained <sup>14</sup>C dates can clearly be regarded as outliers,  
157 all results of radiocarbon dating were included in the modeling performed for Lake Khall.  
158 Additionally, the sampling year AD 2006 was assigned to the depth 0 and AD 1963 at 6.25  
159 cm, identified on the basis of <sup>137</sup>Cs peak. The age-depth model was calculated with 20  
160 sections. The *a priori* information for accumulation rate was set as a gamma distribution with  
161 mean 30 yrs/cm and shape 2, and a beta distribution with strength 4 and mean 0.7 was fixed  
162 for the accumulation variability, following the recommendation by Blaauw and Christen  
163 (2011). The age-depth model resulting from 2640000 iterations is presented in Figure 2.

164 The uppermost 36 cm of sediment were also dated using <sup>210</sup>Pb, a naturally-produced  
165 radionuclide that has been extensively used in the dating of recent sediments (Appleby, 2001)  
166 and <sup>137</sup>Cs, an artificially produced radionuclide, introduced to the study area by atmospheric  
167 fallout from nuclear weapons testing. Core sub-samples were counted on a Canberra well-  
168 type ultra-low background HPGe gamma ray spectrometer to determine the activities of <sup>210</sup>Pb,  
169 <sup>137</sup>Cs and other gamma emitters. Spectra were accumulated using a 16K channel integrated  
170 multichannel analyzer and analysed using the Genie 2000 system. Energy and efficiency  
171 calibrations were carried out using bentonite clay spiked with a mixed gamma-emitting  
172 radionuclide standard, QCYK8163, and checked against an IAEA marine sediment certified  
173 reference material (IAEA 135). The <sup>210</sup>Pb<sub>excess</sub> activity was estimated by subtraction of the  
174 average value of <sup>210</sup>Pb activity in deeper core samples (14 Bq/kg), where total <sup>210</sup>Pb activities  
175 had fallen to virtually constant values and so approximate the “background” or supported  
176 <sup>210</sup>Pb activity. Sediment accretion rates were determined using the Constant Flux, Constant  
177 Sedimentation (CF-CS) model of <sup>210</sup>Pb dating, where the sedimentation rate is given by the

178 slope of the least squares fit for the natural log of the  $^{210}\text{Pb}_{\text{excess}}$  activity versus depth  
179 (Krishnaswami et al., 1971; Robbins, 1978).

180

### 181 3.2 Pollen analysis

182

183 Twenty-nine 1 cm<sup>3</sup> sediments were processed for pollen analysis using standard  
184 laboratory methods, including HCl and KOH treatments, heavy-liquid separation and  
185 subsequent acetolysis (Berglund and Ralska-Jasiewiczowa, 1986). Pollen and spores were  
186 mounted in glycerin and counted using light microscopy at  $\times 400$ – $\times 1000$  magnification.  
187 Identification of fossil pollen and spores was assisted with the use of regional pollen atlases  
188 (Kuprianova and Alyoshina, 1972; Bobrov et al., 1983; Moore et al., 1991) and the reference  
189 collection held at the Institute of the Earth Crust, Irkutsk. Between 176 and 518 terrestrial  
190 pollen grains were counted at each level (304 on average). Relative abundances of individual  
191 taxa were based on the sum of all terrestrial pollen grains. *Haploxylon*-type pine pollen (*Pinus*  
192 *sibirica*, *Pinus pumila*) were separated from *Diploxylon*-type pine pollen (*Pinus sylvestris*)  
193 based on the position of the sacci in polar view. *Pediastrum* coenobia colonies contain  
194 sporopollenin which allowed us to count them alongside pollen (e.g. Nielsen and Sørensen,  
195 1992). *Pediastrum* relative abundances were calculated in relation to the total sum of  
196 terrestrial pollen. We used the pollen-based biome reconstruction method and equation  
197 presented in Prentice et al. (1996) and a regionally approved biome-taxon matrix (Tarasov et  
198 al., 2009; Bezrukova et al., 2010), which assigns all selected pollen taxa to appropriate  
199 biomes. All terrestrial pollen taxa from Lake Khall sediments were assigned to regional plant  
200 functional types (PFTs) and biomes– see Tarasov et al. (2009) for full details. Quantitative  
201 climate reconstructions were performed using best modern analogue (BMA) approach  
202 (Overpeck et al., 1985; Guiot, 1990) previously applied to the Holocene pollen records from  
203 Lake Baikal (Tarasov et al., 2007) and Lake Kotokel (Tarasov et al., 2009). A reference  
204 modern dataset based on the global climate averages (New et al., 2002) and extensive modern  
205 surface pollen data from northern Eurasia, with a good representation of the Lake Baikal  
206 region (see Tarasov et al., 2005 for details). Reconstructions undertaken were annual  
207 precipitation (Pann), mean July temperatures (Tw, also referred to here as mean temperature  
208 of the warmest month), and mean January temperature (Tc, also referred to here as mean  
209 temperature of the coldest month).

210

### 211 3.3 Ostracods

212

213 Forty samples were processed for ostracod determinations. Wet sediment samples  
214 were dispersed in tap water overnight and then gently sieved through a 250  $\mu\text{m}$  mesh. The  
215 coarse residues were dried at 105°C. All of the ostracod shells were picked from these  
216 residues under a low-power binocular microscope using a fine (4/0) moistened paintbrush,  
217 sorted into taxonomic groups and stored in micropalaeontological slides. Results are  
218 expressed in numbers of valves per unit weight of sediment.

219

### 220 3.4 Mineral Magnetism

221

222 At least 1.5 g of freeze-dried sediment from forty-one samples was packed into  
223 plastic magnetism sample pots. Low-frequency and high-frequency magnetic susceptibility  
224 was measured for each sample using a Bartington MS2 Magnetic Susceptibility meter.

225

### 226 3.5 Particle size

227

228 Particle-size analysis was undertaken on the  $< 2$  mm fraction of sediment from 40  
229 samples. In practice, most of the sediment from the core was less than 2 mm diameter, so the  
230 grain-size analyses are essentially bulk-sample determinations. Each sample was dispersed in  
231 water, sieved through a 2 mm mesh and then disaggregated ultrasonically prior to analysis  
232 using a Malvern Mastersizer laser particle-sizer. The results were processed using

233 GRADISTAT (Blott and Pye, 2001). For plotting purposes, we used the grain-size statistics  
234 produced from the Folk and Ward (1957) method.

235

### 236 3.6 X-ray fluorescence (XRF) spectrometry analysis

237

238 Up to 2 g of freeze dried sediment was finely ground and compressed into 25 mm  
239 deep polythene sample pots for XRF analysis of fortyone samples. Samples were subjected to  
240 gamma photons from a silicon (lithium) semi-conductor detector for 240 s each, using a  
241 Spectro Xlab 2000 energy dispersive XRF spectrometer. Calibration was conducted with two  
242 known sediment standards of Buffalo River Sediment.

243

### 244 3.7 Statistical Analyses

245

246 Detrended correspondence analysis (DCA) was initially undertaken to establish the  
247 magnitude of vegetation turnover. Relative abundance data were  $\log(x+1)$  transformed in  
248 order to stabilize species variance and rare species were down-weighted. The axis 1 gradient  
249 length (standard deviation units) was 1.049, indicating that linear ordination techniques were  
250 more appropriate for analyses. Principal components analysis (PCA) with symmetric scaling  
251 of the ordination scores to optimise scaling for both samples and species was undertaken  
252 (Gabriel, 2002). Species data were  $\log(x+1)$  transformed and both species and samples were  
253 centred to give a log-linear contrast PCA, appropriate for closed relative abundance data  
254 (Lotter and Birks, 1993). XRF data were analysed using PCA with samples centred and  
255 standardised. Significance of PC axes were tested with a broken stick model (Jollifer, 1986)  
256 using BSTICK v1.0 (Line and Birks, 1996). Compositional change in the palynological data  
257 ( $\beta$ -diversity) was estimated using detrended canonical correspondence analysis (DCCA) with  
258 the data constrained using dates obtained from the age-depth model (Birks, 2007). All  
259 ordination analyses were undertaken using Canoco v. 4.5 (ter Braak and Šmilauer, 2002).  
260 Monte Carlo permutation tests for temporally ordered data were used to determine  
261 significance levels ( $n = 499$ ). Stratigraphical profiles were constructed using C2 Data  
262 Analysis Version 1.5.1 (Juggins, 2007). Stratigraphical zones for each proxy were delimited  
263 by optimal partitioning (Birks and Gordon, 1985) using the unpublished programme ZONE  
264 (version 1.2) (Juggins, 1991).

265

## 266 4. Results

267

### 268 4.1 Core description and chronology

269

270 The core consisted mainly of homogenous, silty clay sediment between 0 – 76 cm  
271 (colour 5Y-4/1-2), with the bottom sediments (76 – 91 cm; colour 10YR-3/1) packed full of  
272 broken bivalve shells. The age-depth model for Lake Khall shows that the core spans the past  
273 ca. 5.2 cal ka BP (i.e calibrated years before AD 1950, taken as present, are consistently used)  
274 (Fig. 2). Although the sedimentation rate underwent temporal variability, some distinct  
275 sections can be distinguished, for which the sedimentation rate was relatively constant. For  
276 the uppermost section from 0 to 8 cm (ca. 10 cal BP) the average sedimentation rate derived  
277 from the Bacon model was  $1.48 \pm 0.25$  mm/year, which is in accordance with the number  
278 obtained on the basis of  $^{210}\text{Pb}$  measurements ( $1.11 \pm 0.44$  mm/year). The mean accumulation  
279 rate for the section between 8 cm (10 cal BP) and 74 cm (ca. 2.6 cal ka BP) was  $0.36 \pm 0.02$   
280 mm/year. The oldest part of the sediment was characterized by lower sedimentation rate,  
281  $0.16 \pm 0.043$  mm/year.

282

### 283 4.2 Pollen stratigraphy

284

285 Taiga was the dominant biome throughout the sequence (Fig. 3) suggesting the record  
286 reflects the regional ‘forest’ signal rather than only the local ‘steppe’ one. Compositional  
287 turnover in the palynological data was high ( $\beta$ -diversity=1.281), although greatest change

288 occurred between 5.15 – 2.48 cal ka BP, with a very rapid change between 2.75 – 2.48 cal ka  
 289 BP (Fig 6). Between 1.76 – 0.84 cal ka BP there was very little change in vegetation  
 290 composition, but variability increased markedly from ca. AD 1800 to the present. Only PCA  
 291 axis 1 was significant and accounted for 71.1% of variation in the species data. Three zones  
 292 were delimited within the pollen stratigraphy (Fig. 3).

- 293 • Khall-3 (91 – 73.5 cm; 5.15 - 2.61 cal ka BP) was characterised by highest abundances of  
 294 *Betula* sect. *Albae* (25-50%) and *Artemisia* (10-19%). *Pinus sibirica* percentage values,  
 295 initially very high at the very base of the profile (25%), declined abruptly to 3 % and then  
 296 increased to 10-13% again. *Pinus sylvestris* was initially present in only very low  
 297 abundances (3-4%) at the base of the profile and quickly increased, reaching up to 36-  
 298 41% in upper part of this zone. *Picea obovata* and *Alnus fruticosa* reached their highest  
 299 values (up to 5%) in this zone.
- 300 • Khall-2 (73.5 – 13.25 cm; 2.61 – 0.15 cal ka BP [ca. AD 1800]) was dominated by *P.*  
 301 *sylvestris* pollen, with values fluctuating between 60-84%. *P. sibirica* was also well  
 302 represented (10-25%), and contribution from *Artemisia* varied between 0.5-9%. *Alnus*  
 303 *fruticosa* pollen was absent or present in low abundances. *Picea* percentages were also  
 304 generally low and did not exceed 3%.
- 305 • Khall-1 (13.25 - 0 cm; ca. AD 1800 – AD 2006) had a pollen composition similar to  
 306 Khall-2, with slightly lower and fluctuating percentage values of *P. sylvestris* and slightly  
 307 higher abundances of *B. sect. Albae* and Cyperaceae pollen. Within this zone *Pediastrum*  
 308 algae spores appeared for the first time in the record, and rapidly increased to very high  
 309 abundances.

310

#### 311 4.3 Ostracods

312

313 We only present preliminary results here: detailed taxonomic and palaeoecological  
 314 accounts of the ostracod assemblages will follow in a future publication. The ostracod  
 315 assemblages were fairly low diversity (<10 species in total) and dominated by a member of  
 316 the genus *Limnocythere*, which has yet to be identified to specific level (Fig. 4). Other taxa  
 317 present include *Candona* spp., *Pseudocanadona* spp., *Cyclocypris* sp., *Cypris* sp., *Ilyocypris*  
 318 sp. and *Potamocypris* sp. as well as several others that remain unidentified. In most of the  
 319 core levels examined, adult and juvenile shells were found. Concentrations varied from about  
 320 300 to less than 2 valves per gram of sediment. Concentrations were greatest in the basal 10  
 321 cm of the core, declining above this. Candonids were absent above 2.10 cal ka BP. A varying  
 322 proportion of the valves displayed a black coating. Energy dispersive spectroscopy (EDS)  
 323 analysis under a scanning electron microscope suggested that the coating was non-metallic  
 324 but laser Raman determinations were inconclusive.

325

#### 326 4.4 Mineral Magnetism

327

328 Low field magnetic susceptibility measurements ranged between 0.1 - 4.7 10<sup>-5</sup> SI  
 329 (Fig. 5). Values increased by small amount from the base of the core up to ca. 2.8 cal ka BP  
 330 (2 – 2.6 10<sup>-5</sup> SI). There was a substantial increase in values between ca. 2.6 – 2.1 cal ka BP  
 331 from 2.6 – 4.3 10<sup>-5</sup> SI. Values showed almost no change between 1.4 – 1.0 cal ka BP, after  
 332 which they declined to the top of the profile, with very rapid decline after AD 1800.

333

#### 334 4.5 Particle Size

335

336 Mean particle size (Mz;  $\mu\text{m}$ ) ranged between 12.7 – 48.3  $\mu\text{m}$ ) (mean = 20.6; median  
 337 17.6). Five peaks greater than mean Mz occurred at 5.12, 2.52, 1.88, 0.79 cal ka BP and AD  
 338 1925 (Fig 5). Sorting of the grain size distributions ranged between 3.2 and 7.1  $\mu\text{m}$  (mean =  
 339 3.9; median 3.7). Five sorting peaks greater than the mean occurred at identical times as peaks  
 340 in Mz. Almost all skewness values were negative (mean = -0.1; median = -0.1), except for 5  
 341 positive values that occurred at the same times as high values for mean grain size and sorting.



342 Kurtosis (mean = 1.0; median = 1.0) exhibited a different pattern from other grain size  
343 parameters. Values were above average between 5.12 – 3.03 cal ka BP, and declined to lowest  
344 value at 2.52 cal ka BP, when values of other particle size proxies increased. But peaks in  
345 kurtosis did co-occur at 1.88, 0.79 cal ka BP and 1925 AD.

#### 346 347 4.6 XRF spectrometry analysis 348

349 Selected elements are presented in Figure 7. Ti, Al and K increased from 5.08 cal -  
350 1.80 cal ka BP. Between 1.80 – 0.80 cal ka BP values showed little variation, and then they  
351 declined up to ca. AD 1950. The rate of decline increased at the top of zone Khall-2, from  
352 0.12 ka BP, concomitant with rapid increase in sedimentation rate and decline in magnetic  
353 susceptibility values. Only PCA axis 1 was significant, accounting for 73.8% of variance in  
354 geochemical data. This axis was driven by a strong gradient between high Ca and Sr  
355 concentrations at the bottom of the core, and high concentrations of most other elements  
356 between ca. 1.90 – 0.50 cal ka BP (notably Fe, Y, Zn, Rb, K, Ti, Cu and Al) (Fig. 6).  
357 Although axis 2 was insignificant, elevated concentrations of S and Cl were especially  
358 abundant in the uppermost sediments.  
359

### 360 361 5. Discussion 362

363 Taiga biome dominated the vegetation reconstruction from the Ol'khon region since  
364 at least 5.2 ka BP. However, compositional turnover was very significant;  $\beta$ -diversity values  
365 were considerably higher than for longer Holocene sequences in other boreal regions such as  
366 southern Norway (Birks, 2007) and the eastern Sayan Mountains (Mackay et al., 2012). This  
367 suggests that the semi-arid, Ol'khon region was more sensitive to climate variability and  
368 environmental change than other boreal regions with higher precipitation. Such sensitivity  
369 was responsible for major directional shifts during the past 5.2 cal ka in Lake Khall and the  
370 surrounding region. DCCA and zonation analyses delimited most rapid periods of vegetation  
371 change at 2.74 – 2.48 cal ka and after AD 1800. Pollen assemblage composition showed a  
372 progressive decrease in birch pollen and shift to a predominance of Scots pine pollen between  
373 5.15–2.48 cal ka, which drove overall compositional turnover. Scots pine produces vast  
374 amounts of pollen, and once established, it dominates pollen assemblages. The numerical  
375 scores of the taiga biome (Fig. 3) demonstrated minor fluctuations, but did not show  
376 decreasing or increasing trend through the whole record. Therefore, the increase in arboreal  
377 pollen percentages between 2.75 – 2.48 cal ka BP likely does not imply greater regional  
378 afforestation, nor any decrease in steppe communities, but are indicative of change in forest  
379 composition, with the spread of eurythermic and drought resistant Scots pine rather than  
380 noticeable spread in regional woody cover. These findings are in line with the woody cover  
381 reconstruction derived from Lake Kotokel pollen records on the opposite shore of Lake  
382 Baikal (Fig. 1) (Tarasov et al., 2009; Bezrukova et al., 2010).  
383

#### 384 5.1 Mid-Holocene environmental change 385

386 Up to 4.5 cal ka BP, forest-steppe communities dominated local vegetation in  
387 Ol'khon region, especially tree birches (*Betula* sect. *Albae*), *Artemisia* and *Chenopodiaceae*  
388 taxa. Reconstructed temperature of the coldest month and annual precipitation were highest  
389 during this period. Owing to the lack of formal identification of the ostracod species,  
390 interpretations of the assemblages remain circumspect at this stage, although we can say that  
391 assemblages were deposited *in situ*, because in most of the core levels examined, both adult  
392 and juvenile shells were found. However, candonids generally only tolerate low salinity  
393 waters (Holmes et al., 2010) and the Lake Khall assemblage suggests that the lake was fresher  
394 in the past. The geochemical record also provides evidence for a fresher lake in the past; low  
395 Sr/Ca ratios indicate low lake-water salinity (Marshall, 1969). Detrital transport from the  
396 catchment into the lake are represented by e.g. Ti, Al and K, and these elements were lowest

397 when precipitation was highest. Ca on the other hand may come from both authigenic  
398 production within the lake and from detrital flux (e.g. Wünnemann et al., 2010). In order to  
399 distinguish between these two processes we use the Ca/Al ratio, which at the base of the core  
400 was very high (60), indicative of high authigenic production. High production occurs at the  
401 same time as highest concentrations of ostracods, and shell remains of a, as yet unidentified,  
402 bivalve. We have as yet to characterise mineralogy of the sediments (e.g. using XRD) but low  
403 K/Rb and high Ti/K ratios suggest dominance of clays and micas, although feldspars became  
404 more important after 3.59 cal ka BP. Elsewhere in the Lake Baikal region, other records of  
405 pollen-inferred annual precipitation were also high (e.g. Tarasov et al., 2007; Tarasov et al.,  
406 2009), as was isotopic evidence for elevated precipitation-dominated discharge into Lake  
407 Baikal (Mackay et al., 2011; Fig 8). Further afield, isotopic records from Dongge Cave in  
408 southern China (Fig 8) were indicative of strong East Asian Summer Monsoon (EASM)  
409 linked to relative high summer insolation (Wang et al., 2005).

410 Between ca. 4.4 – 2.8 cal ka BP, the pollen record is poorly resolved. However, there  
411 was a significant expansion of Scots pine (*P. sylvestris*) and, to a lesser extent, Siberian pine  
412 (*P. sibirica*) (a major component of dark, coniferous taiga), concomitant with a decline in  
413 deciduous forest. The expansion of Scots pine occurred substantially later than at  
414 neighbouring regions e.g. Lake Hovsgöl (10.0 cal ka BP; Prokopenko et al., 2007), Altai  
415 Mountains, (9.5 cal ka BP, Blyakharchuk et al., 2004), Eastern Sayan Mountains (9.1 cal ka  
416 BP, Mackay et al., 2012), southern Lake Baikal (7 cal ka BP, Demske et al., 2005) and Lake  
417 Kotokel (ca. 6.9 - 6.4 cal ka BP (Bezrukova et al., 2008; Shichi et al., 2009). The expansion  
418 of Scots pine in Ol'khon is in close agreement with the expansion of Scots pine to the north of  
419 Lake Baikal (5.2 cal ka BP, Bezrukova et al., 2006), highlighting that distinct regional  
420 differences exist in the spread of conifer forest to coastal regions of Lake Baikal. The period  
421 of conifer expansion in Ol'khon region occurred during a period of increasing aridity, as  
422 inferred from several of the proxies studied. For example, Sr/Ca ratios indicate a progressive  
423 increase in salinity of Lake Khall, likely linked to reductions in pollen-inferred precipitation  
424 anomalies, while pollen-inferred temperatures remained above values experienced in recent  
425 decades (Fig. 8). Detrital input (inferred from Al, Ti and K) also increased at this time. Given  
426 the similarity between PCA of the vegetation and geochemistry, it is likely that both were  
427 influenced by the same drivers. Elsewhere,  $\delta^{18}\text{O}_{\text{diatom}}$  showed a marked decline during this  
428 period, indicative of a decline in the proportion of rain-fed discharge into Lake Baikal  
429 (Mackay et al., 2011; Fig. 8). The shift to a more arid climate was also reflected further afield  
430 in the weakening of the EASM (Wang et al., 2005; Fig. 8).

431

## 432 5.2 Abrupt environmental change

433

434 Compositional turnover in vegetation communities was greatest between 2.75 – 2.48  
435 cal ka BP, which continued to change up to 1.87 cal ka BP, linked to the maximum expansion  
436 of dark coniferous taiga. Particle size characteristics in Lake Khall show that they were  
437 generally very poorly sorted, i.e. they had not undergone efficient sorting before their burial  
438 into the bottom sediments, which is common for shallow lakes (Mischke et al., 2010). One of  
439 the largest peaks in mean particle size occurred at 2.52 cal ka BP, which was likely caused by  
440 strong aeolian influx because these large particles were also extremely unsorted (Fig. 5).  
441 Pollen-inferred annual precipitation anomalies dropped rapidly, and values remained low,  
442 below that of the present day, for much of the remainder of the Holocene (Fig. 8). There was  
443 also a marked decline in mean temperature of coldest month, while mean temperatures of the  
444 warmest month increased. The climate in the Ol'khon region therefore became more  
445 continental. The start of these climatic and vegetation changes are coincident with a peak in  
446 ice rafted debris material in North Atlantic sediments (IRD-2; Bond et al. 1997), which also  
447 resulted in low  $\delta^{18}\text{O}$  isotopic values in Lake Baikal and in Dongge cave, indicative of a  
448 decline in proportion of rain-fed discharge into Lake Baikal (Mackay et al., 2011) and an  
449 attenuated EASM (Wang et al., 2005) respectively.

450 Between 2.12 – 1.87 cal ka BP there was a significant decline in mean annual  
451 precipitation and mean temperature of the coldest month but an increase in mean temperature

452 of the warmest month (Fig 8). Drier, more continental climate resulted in peak abundance of  
453 Scots pine, which drove compositional turnover in the Ol'khon region. An increase in Sr/Ca  
454 ratio suggested that chemical composition of the groundwater that feeds Lake Khall may have  
455 become more saline, and this event may have caused the final decline in substantial numbers  
456 of the ostracod *Candona* sp. Therefore it seems likely that the region underwent a period of  
457 extreme drought, which led to a decline in ostracoda in general. The rapid increase in  
458 sedimentation rate was concurrent with small peaks in particle size, perhaps indicative of  
459 increased aeolian transport onto the lake.

460

### 461 5.3 Late Holocene variability

462

463 Between ca. 1.9 – 0.7 cal ka BP, taxa indicative of cold coniferous forest declined and  
464 steppe communities virtually disappeared from the record altogether, coincident with marked  
465 increases in warmest month temperature anomalies. This period in general was characterised  
466 by little vegetation compositional change, and stable input of catchment derived particles  
467 (Figs. 3, 5, 7). Increased reconstructed summer and winter temperatures were likely linked to  
468 increased northern hemisphere temperatures, as inferred from the GRIP borehole (Dahl-  
469 Jensen et al., 1998) (Fig. 8). Elsewhere in the Lake Baikal region, steppe communities were  
470 also less common (Tarasov et al., 2007), while high biogenic silica concentrations within  
471 Lake Baikal sediments were indicative of high aquatic productivity (Prokopenko et al., 2007).  
472 Peak reconstructed summer temperatures occurred between 1.33 – 0.77 cal ka BP, coincident  
473 with the period known as both the Medieval Warm Period (MWP) and Medieval Climate  
474 Anomaly (MCA). This period is distinct because although temperatures in many regions were  
475 warm (Mann et al., 2009) precipitation anomalies were also apparent in many regions in the  
476 world (Stine, 1994), leading to severe drought in e.g. northern Europe (Helama et al., 2009)  
477 and North America (Seager and Burgman, 2011). In the Ol'khon region, precipitation  
478 anomalies were higher than the previous period of drought, but still lower than the present.  
479 One of the few stratified deposits in the Lake Baikal region was excavated at Sagan-Zaba and  
480 dated between 2.0 – 0.9 cal ka BP. These deposits were likely associated with pastoralists,  
481 and although we are not able to say if the evidence of pastoralism was linked to a particularly  
482 quiescent period of environmental change, warmer summer and milder winter temperatures  
483 may have been conducive to a pastoral way of life.

484

485 For a short period between ca. 0.77 – 0.45 cal ka BP, local climate in the Ol'khon  
486 region became wetter and substantially colder, leading to an increase in *P. sibirica*, *Picea*  
487 *obovata* and sedge pollen. *P. obovata* (Siberian spruce) is characteristic of soils with elevated  
488 moisture content, and likely represents real increases in tree abundance close to the lake  
489 (Bezrukova et al., 2005). However, there did not appear to be a substantial influence on Lake  
489 Khall itself – Sr/Ca ratios continued to increase, while ostracods only showed small increases  
490 in concentration. It is noteworthy that candonids did not recolonise the lake in any substantial  
491 numbers, and that black coatings on the ostracod valves almost disappeared. On the basis of  
492 the EDS and laser Raman determinations detailed in section 4.3, it was assumed that the  
493 coatings were organic and indicative of reducing conditions in the upper layers of the  
494 sediment following death of the ostracods. Blackened valves dominated the lower part of the  
495 core, and were less common above 0.68 cal ka BP, suggesting a significant change in the  
496 ventilation of the lake after this time. Further work still needs to be done to determine the  
497 nature of the black coatings. Wetter climate has also been reconstructed from peat bog  
498 sequences from the northern shore of Lake Baikal (Bezrukova et al., 2006), and further afield  
499 in the Eastern Sayan mountains (Mackay et al. 2012). This period is coincident with IRD0 in  
500 North Atlantic sediments and attenuation of the EASM (Wang et al., 2005; Fig 8), and is  
501 concurrent with the Little Ice Age. Young moraines, associated with re-advancing glaciers at  
502 this time, can be found in the Sayan Mountains (Ivanovsky and Panychev, 1978 in  
503 Shahgedanova et al., 2002), indicative of cooler, regional environments (Krenke and  
504 Chernavskaya, 2002). Chironomid-inferred temperatures from lake ESM-1 in the Eastern  
505 Sayan Mountains also showed a distinct cooling (Mackay et al., 2012).

506 Since ca. AD 1845, the increase in deciduous forest was linked to increased pollen-  
507 inferred precipitation and pollen-inferred temperature anomalies of the coldest and warmest  
508 months. The most striking change in the palynological record however, is the rapid increase  
509 in *Pediastrum* algae. *Pediastrum* belongs to the Chlorophyceae green algae, and is often  
510 characteristic of more nutrient rich waters. Palaeoenvironmental interpretations from  
511 *Pediastrum* records in lake sediments are not straightforward. Several studies tie the presence  
512 of *Pediastrum* to high lake levels in the semi-arid regions of e.g. Inner Mongolia (Jiang et al.,  
513 2006) and NE Tibetan Plateau (Zhao et al., 2007). In southern Scandinavia, increased  
514 concentrations of *Pediastrum* coenobia occurred during periods of warmer climate and  
515 increased lacustrine productivity (Sarmaja-Korjonen et al., 2006; Panizzo et al., 2008). In  
516 Lake Khall, increasing *Pediastrum* was coincident with increases in temperature of the  
517 coldest month and annual precipitation. During this period there was a rapid increase in  
518 sediment accumulation rate, the fastest for the past 5 ka, concomitant with a rapid decline in  
519 low field initial magnetic susceptibility measurements. This suggests that there was a decline  
520 in magnetisable sediments, possibly related to increased organic content and presence of algal  
521 growth. The increase in *Pediastrum* sp. therefore is likely indicative of a more nutrient rich  
522 lake. Animal husbandry intensified in the Lake Baikal region at this time because of the  
523 influx of Russian populations (Tarasov et al., 2007). Local populations later undertook tree-  
524 felling (Sizykh, 2007), and although there is limited pollen evidence of anthropogenic  
525 activities, impacts on lacustrine ecosystems could be expected.

## 526 527 **6. Conclusions**

528  
529 A multiproxy study of a small, shallow lake in the Ol'khon region of Lake Baikal was  
530 undertaken to determine climatic and human impacts on the landscape over the mid- to late-  
531 Holocene. We could only relate the significant turnover in vegetation composition to climate  
532 variability, and we found no evidence for anthropogenic activity despite the region having a  
533 long history of pastoralism. Geochemical evidence suggested that Lake Khall was once more  
534 fresh than it is today, and that over the study period, groundwater feeding the lake became  
535 more saline. The change in chemical composition had a negative impact on aquatic fauna by 2  
536 cal ka BP. Pollen based reconstructions from Lake Kotokel, a satellite to Lake Baikal  
537 (Tarasov et al., 2009) and regional climate modelling (White and Bush, 2010) exhibited  
538 similar trends to reconstructions from Lake Khall. For example, general trends demonstrated  
539 a decline in atmospheric precipitation and increase in continentality. The decrease in  
540 precipitation was accompanied by the changes in its seasonality, i.e. late Holocene  
541 strengthening of Westerlies in the region caused relative increase in winter (snow)  
542 accumulation. This feature together with drier summer conditions favoured the spread of  
543 drought resistant Scots pine. Reconstructed cool, moist conditions during the Little Ice Age  
544 are consistent with other palaeolimnological records, highlighting the regional nature of the  
545 response. Proxy records from Lake Khall also show a period of relative stability concurrent  
546 with the Medieval Climate Anomaly and a period of abrupt change between 2.75 – 2.48 cal  
547 ka BP, concurrent with influence from IRD-2 event in the north Atlantic. Finally, although  
548 human impact could not be determined from the terrestrial pollen record, preserved  
549 *Pediastrum* colonies may be indicative of a major recent phase of human impact as numbers  
550 of pastoralists migrated into the region in the last 100 years.

## 551 552 **Acknowledgements**

553 We gratefully acknowledge funding through the Baikal Archaeology Project,  
554 supported by the Major Collaborative Research Initiative (MCRI) programme of the Social  
555 Sciences and Humanities Research Council of Canada. Thanks are given to Cath D'Alton for  
556 help in preparing figures and to Holly Watson for undertaking magnetic susceptibility  
557 measurements and particle size analysis.

560  
561  
562  
563  
564  
565  
566  
567  
568  
569  
570  
571  
572  
573  
574  
575  
576  
577  
578  
579  
580  
581  
582  
583  
584  
585  
586  
587  
588  
589  
590  
591  
592  
593  
594  
595  
596  
597  
598  
599  
600  
601  
602  
603  
604  
605  
606  
607  
608  
609  
610  
611  
612  
613

## References

- Appleby, P.G., 2001. Chronostratigraphic techniques in recent sediments. In: Last, W.M., Smol, J.P. (Eds.) *Tracking Environmental Change Using Lake Sediments, Volumes 1*. Kluwer, Dordrecht, pp. 171-203
- Atlas Baikala (Baikal Atlas) 1993. Federal Service of Surveying and Cartography, Moscow. 159 pp. In Russian.
- Berger A., Loutre M.F., 1991. Insolation values for the climate of the last 10 million years. *Quaternary Science Reviews* 10, 297-317.
- Berglund, B.E., Ralska-Jasiewiczowa, M., 1986. Pollen analysis and pollen diagrams. In: Berglund, B.E. (Ed.), *Handbook of Holocene Palaeoecology and Palaeohydrology*, Interscience, New-York, pp. 455-484.
- Bezrukova, E.V., Abzaeva, A.A., Letunova, P.P., Kulagina, N.V., Vershinin, K.E., Belov, A.V., Orlova, L.A., Danko, L.V., Krapivina, S.M., 2005. Post-glacial history of Siberian spruce (*Picea obovata*) in the Lake Baikal area and the significance of this species as a paleo-environmental indicator. *Quaternary International* 136, 47-57.
- Bezrukova, E.V., Belov, A.V., Abzaeva, A.A., Letunova, P.P., Orlova, L.A., Sokolova, L.P., Kalugina, N.V., Fisher, E.E., 2006. First high-resolution dated records of vegetation and climate changes on the Lake Baikal northern shore in the middle-late Holocene. *Doklady Earth Sciences* 411, 1331-1335.
- Bezrukova, E.V., Krivonogov, S.K., Takahara, H., Letunova, P.P., Shichi, K., Abzaeva, A.A., Kalugina, N.V., Zabelina, Yu, S., 2008. Lake Kotokel as a stratotype for the Lake Glacial and Holocene southeastern Siberia. *Doklady Earth Sciences* 420, 658-663.
- Bezrukova, E.V., Tarasov, P.E., Solovieva, N., Krivonogov, S.K., Fiedal, F., 2010. Last glacial-interglacial vegetation and environmental dynamics in southern Siberia: chronology, forcings and feedbacks. *Palaeogeography, Palaeoclimatology, Palaeoecology* 296, 185-198.
- Birks, H.J.B., 2007. Estimating the amount of compositional change in late-Quaternary pollen stratigraphical data. *Vegetation History and Archaeobotany* 16, 197-202.
- Birks, H.J.B., Gordon, A.D., 1985. *Numerical methods in Quaternary pollen analysis*. Academic Press, London.
- Blaauw, M., Christen, J.A., 2011. Flexible paleoclimate age-depth models using an autoregressive gamma process. *Bayesian Analysis* 6, 457-474.
- Blott, S.J., Pye, K., 2001. GRADISTAT: a grain size distribution and statistics package for the analysis of unconsolidated sediments. *Earth Surface Processes and Landforms* 26, 1237-1248.
- Blyakharchuk, T.A., Wright, H.E., Borodavko, P.S., van der Knaap, W.O., Amman, B., 2004. Late Glacial and Holocene vegetational changes on the Ulagan high-mountain plateau, Altai Mountains, southern Siberia. *Palaeogeography, Palaeoclimatology and Palaeoecology* 209, 259-279.
- Bobrov, A.E., Kuprianova, L.A., Litvintseva, M.V., Tarasevich, V.F., 1983. *Sporae Pteridophytorum et Pollen Gymnospermarum Monocotyledonearumque. Florae Parties Europaeae USSR*. Nauka, Leningrad. (in Russian).
- Bond, G., Showers, W., Cheseby, M., Lotti, R., Almasi, P., deMenocal, P., Priore, P., Cullen, H., Hajdas, I., Bonani, G., 1997. A pervasive millennial scale cycle in North Atlantic Holocene and glacial climates. *Science* 278, 1257-1256.
- Bronk Ramsey, C., 2009. Bayesian analysis of radiocarbon dates. *Radiocarbon* 51, 337-360.
- Dahl-Jensen, D., Mosegaard, K., Gundestrup, N., Clow, G.D., Johnsen, S.J., Hansen, A.W., Balling, N., 1998. Past temperatures directly from the Greenland Ice Sheet. *Science* 282, 268-271.
- Demske, D., Heumann, G., Granoszewski, W., Nita, M., Mamakowa, K., Tarasov, P.E., Oberhänsli, H., 2005. Late glacial and Holocene vegetation and regional climate variability evidenced in high-resolution pollen records from Lake Baikal. *Global and Planetary Change* 46, 255-279.

- 614 Folk, R.L., Ward, W.C., 1957. Brazos River bar: a study in the significance of grain size  
615 parameters. *Journal of Sedimentary Petrology* 27, 3-26.
- 616 Gabriel, K.R., 2002. Goodness of fit of biplots and correspondence analysis. *Biometrika* 89,  
617 423-436.
- 618 Goslar T., Czernik J., Goslar E., 2004. Low-energy <sup>14</sup>C AMS in Poznan radiocarbon  
619 Laboratory, Poland. *Nuclear Instruments and Methods in Physics Research B*, 223-  
620 224, 5-11.
- 621 Guiot, J., 1990. Methodology of the last climatic cycle reconstruction from pollen data.  
622 *Palaeogeography, Palaeoclimatology, Palaeoecology* 80, 49–69.
- 623 Helama, S., Merilainen, J., Tuomenvirta, H., 2009. Multicentennial megadrought in northern  
624 Europe coincided with a global El Niño-Southern Oscillation drought pattern during  
625 the Medieval Climate Anomaly. *Geology* 37, 175-178.
- 626 Holmes, J., Sayer, C.D., Liptrot, E., Hoare, D.J., 2010. Complex controls on ostracod  
627 palaeoecology in a shallow coastal brackish-water lake: implications for  
628 palaeosalinity reconstruction. *Freshwater Biology* 55, 2484-2498.
- 629 Jacobson, G.L., Jr, Bradshaw, R.H.W., 1981. The selection of sites for paleovegetational  
630 studies. *Quaternary Research* 16, 80–96.
- 631 Jiang, W.Y., Guo, Z.T., Sun, X.J., Wu, H.B., Chu, G.Q., Yuan, B.Y., Hattée, C., Guiot, J.,  
632 2006. Reconstruction of climate and vegetation changes of Lake Bayanchagan (Inner  
633 Mongolia): Holocene variability of the East Asian monsoon. *Quaternary Research* 65,  
634 411–420.
- 635 Jolliffe, I.T., 1986. *Principal components analysis*. Springer-Verlag, New York.
- 636 Juggins, S., 1991. ZONE, Version 1.2. University of Newcastle, Newcastle Upon Tyne, UK.
- 637 Juggins, S., 2007. C2 Version 1.5.1 Software for ecological and palaeoecological data  
638 analysis and visualisation. Newcastle University, Newcastle upon Tyne, UK.
- 639 Krenke, A.N., Chernavskaya, M.M., 2002. Climate changes in the preinstrumental period of  
640 the last millennium and their manifestations over the Russian Plain. *Izvestiya,*  
641 *Atmospheric and Oceanic Physics* 38, S59-S79.
- 642 Krishnaswami, S., Lal, D., Martin, J.M., Meybeck, M., 1971. Geochronology of lake  
643 sediments. *Earth and Planetary Science Letters* 11, 407-414.
- 644 Kuprianova, L.A., Alyoshina, L.A., 1972. Pollen and spores of the plants of the flora of the  
645 European part of USSR. Nauka, Leningrad (in Russian).
- 646 Line, J.M., Birks, H.J.B., 1996. BSTICK Version 1.0. Unpublished computer program.  
647 Botanical Institute, University of Bergen, Bergen.
- 648 Lotter, A.F., Birks, H.J.B., 1993. The impact of the Laacher See tephra on terrestrial and  
649 aquatic ecosystems in the Black Forest, southern Germany. *Journal of Quaternary*  
650 *Science* 8, 263-276.
- 651 Mackay, A.W., Swann, G.E.A., Brewer, T., Leng, M.J., Morley, D.W., Piotrowska, N.,  
652 Rioual, P., White, D., 2011. A reassessment of Lateglacial–Holocene diatom oxygen  
653 isotope records from Lake Baikal using a mass balance approach. *Journal of*  
654 *Quaternary Science* 26, 627-634.
- 655 Mackay, A.W., Bezrukova, E.V., Leng, M.J., Meaney, M., Nunes, A., Piotrowska, N., Self,  
656 A., Shchetnikov, A., Shilland, E., Taarasov, P., Wang, L., White, D., 2012. Aquatic  
657 ecosystem responses to Holocene climate change and biome development in boreal  
658 central Asia. *Quaternary Science Reviews* 41, 119-131.
- 659 Mann, M.E., Zhang, Z., Rutherford, S., Bradley, R.S., Hughes, M.K., Shindell, D., Ammann,  
660 C., Faluvegi, G., Ni, F., 2009. Global signatures and dynamical origins of the Little  
661 Ice Age and Medieval Climate Anomaly. *Science* 326, 1256-1260.
- 662 Marshall, F.C., 1969. Lower and Middle Pennsylvanian Fusulinids from the Bird Spring  
663 Formation near Mountain Springs Pass, Clark County, Nevada. *Brigham Young*  
664 *University Geology Studies* 16, 97-154.
- 665 Mischke, S., Zhang, C., Börner, A., Herzschuh, U., 2010. Lateglacial and Holocene variation  
666 in Aeolian sediment flux over the northeastern Tibetan Plateau recorded by laminated  
667 sediments of a saline meromictic lake. *Journal of Quaternary Science* 25, 162-177.
- 668 Moore, P.D., Webb, J.A., Collinson, M.E., 1991. *Pollen Analysis*. Blackwell Scientific

669 Publications, Osney Mead, Oxford.

670 Müller, G., Iron, G., Forstner, U., 1972. Formation and diagenesis of inorganic Ca-Mg  
671 carbonates in the lacustrine environment. *Naturwissenschaften* 59, 158–64.

672 New, M., Lister, D., Hulme, M., Makin, I., 2002. A high-resolution data set of surface climate  
673 over global land areas. *Climate Research* 21, 1–25.

674 Nielsen, H., Sørensen, I., 1992. Taxonomy and stratigraphy of lateglacial *Pediastrum* taxa  
675 from Lysmosen, Denmark – a preliminary study. *Review of Palaeobotany and*  
676 *Palynology* 74, 55–75.

677 Nomokonova, T., Losely, R.J., Goriunova, O.I., Weber, A., (in review). A freshwater old  
678 carbon offset in Lake Baikal, Siberia and problems with the radiocarbon dating of  
679 archaeological sediments: evidence from the Sagan Zaba II site. *Quaternary*  
680 *International*

681 Nomokonova, T., Losely, R.J., Weber, A., Goriunova, L.I., Novikov, A.G., 2010. Late  
682 Holocene subsistence practices among cis-Baikal pastoralists, Siberia:  
683 zooarchaeological insights from Sagan-Zaba II. *Asian Perspectives* 49, 157-179.

684 Overpeck, J.T., Webb III, T., Prentice, I.C., 1985. Quantitative interpretation of fossil pollen  
685 spectra, dissimilarity coefficients and the method of modern analogs. *Quaternary*  
686 *Research* 23, 87–108.

687 Panizzo, V.N., Jones, V.J., Birks, H.J.B., Boyle, J.F., Brooks, S.J., Leng, M.J., 2008. A  
688 multiproxy palaeolimnological investigation of Holocene environmental change,  
689 between c. 10 700 and 7200 years BP, at Holebudalen, southern Norway. *The*  
690 *Holocene* 18, 805-817.

691 Prentice, I.C., Guiot, J., Huntley, B., Jolly, D., Cheddadi, R., 1996. Reconstructing biomes  
692 from palaeological data: a general method and its application to European pollen  
693 data at 0 and 6 ka. *Climate Dynamics* 12, 185–194.

694 Prokopenko, A.A., Khursevich, G.K., Bezrukova, E.V., Kuzmin, M.I., Boes, X., Williams,  
695 D.F., Fedenya, S.A., Kulagina, N.V., Letunova, P.P., Abzaeva, A.A., 2007.  
696 Paleoenvironmental proxy records from Lake Hovsgol, Mongolia, and a synthesis of  
697 Holocene climate change in the Lake Baikal watershed. *Quaternary Research* 68, 2-  
698 17.

699 Ptitsyn, A.B., Reshetova, S.A., Babich, V.V., Daryin, A.V., Kalugin, I.A., Ovchinnikov,  
700 D.V., Panizzo, V., Myglan, V.S., 2010. Palaeoclimate chronology and aridization  
701 tendencies in the Transbaikalia for the last 1900 years. *Geography and Natural*  
702 *Resources* 31, 144-147.

703 Reimer, P.J., Baillie, M.G.L., Bard, E., Bayliss, A., Beck, J.W., Blackwell, P.G., Bronk  
704 Ramsey, C., Buck, C.E., Burr, G.S., Edwards, R.L., Friedrich, M., Grootes, P.M.,  
705 Guilderson, T.P., Hajdas, I., Heaton, T.J., Hogg, A.G., Hughen, K.A., Kaiser, K.F.,  
706 Kromer, B., McCormac, F.G., Manning, S.W., Reimer, R.W., Richards, D.A.,  
707 Southon, J.R., Talamo, S., Turney, C.S.M., van der Plicht, J., Weyhenmeyer, C.E.,  
708 2009. IntCal09 and Marine09 radiocarbon age calibration curves, 0–50,000 years cal  
709 BP. *Radiocarbon* 51, 1111–50.

710 Robbins, J.A., 1978. Geochemical and geophysical applications of radioactive lead. In:  
711 Nriagu, J.O. (Ed.) *Biogeochemistry of Lead in the Environment*. Elsevier Scientific,  
712 Amsterdam, 285-393.

713 Sarmaja-Korjonen, K., Seppänen, A., Bennike, O., 2006. *Pediastrum* algae from the classic  
714 late glacial Bølling Sø site, Denmark: response of aquatic biota to climate change.  
715 *Review of Palaeobotany and Palynology* 138, 95–107.

716 Seager, R., Burgman, R.J., 2011. Medieval hydroclimate revisited. *PAGES news* 19, 10-12.

717 Seppä, H., Bennett, K.D., 2003. Quaternary pollen analysis: recent progress in palaeoecology  
718 and palaeoclimatology. *Progress in Physical Geography* 27, 548-579.

719 Shahgedanova, M., Mikhailov, N., Larin, S., Bredikhin, A., 2002. The mountains of southern  
720 Siberia. In: Shahgedanova, M. (Ed.) *The Physical Geography of Northern Eurasia*.  
721 OUP, Oxford, pp 314-349.

- 722 Shichi, K., Takahara, H., Krivonogov, S.K., Bezrukova, E.V., Kashiwaya, K., Takehara, A.,  
723 Nakamura, T., 2009. Late Pleistocene and Holocene vegetation and climate records  
724 from Lake Kotokel, central Baikal region. *Quaternary International* 205, 98-110.
- 725 Sizykh, A.P., 2007. Models of taiga-steppe communities on the western coast of Lake Baikal.  
726 *Russian Journal of Ecology* 38, 234-237
- 727 Sklyarov, E.V., Solotchina, E.P., Vologina, E.G., Ignatova, N.V., Izokh, O.P., Kulagina,  
728 N.V., Sklyarova, O.A., Solotchin, P.A., Stolpovskaya, V.N., Ukhova, N.N.,  
729 Federovskii, V.S., Khlystov, O.M., 2010. Detailed Holocene climate record from the  
730 carbonate section of saline Lake Tsagan-Tyrm (West Baikal area). *Russian Geology  
731 and Geophysics* 51, 237-258.
- 732 Sklyarova, O.A., Sklyarov, E.V., Fedorovskii, V.S., 2002. Structural control of location and  
733 water chemistry of lakes and springs in the Ol'khon region. *Russian Geology and  
734 Geophysics* 43, 732-745.
- 735 Stine, S., 1994. Extreme and persistent drought in California and Patagonia during Medieval  
736 time. *Nature* 369, 546-549.
- 737 Sugita, S., 1994. Pollen representation of vegetation in Quaternary sediments: theory and  
738 method in patchy vegetation. *Journal of Ecology* 82, 881-97.
- 739 Tarasov, P., Granoszewski, W., Bezrukova, E., Brewer, S., Nita, M., Abzaeva, A.,  
740 Oberhänsli, H., 2005. Quantitative reconstruction of the Last Interglacial vegetation  
741 and climate based on the pollen record from Lake Baikal, Russia. *Climate Dynamics*  
742 25, 625-637.
- 743 Tarasov, P., Bezrukova, E., Karabanov, E., Nakagawa, T., Wagner, M., Kulagina, N.,  
744 Letunova, P., Abzaeva, A., Granoszewski, W., Riedel, F., 2007. Vegetation and  
745 climate dynamics during the Holocene and Eemian interglacials derived from Lake  
746 Baikal pollen records. *Palaeogeography, Palaeoclimatology and Palaeoecology* 252,  
747 440-457.
- 748 Tarasov, P.E., Bezrukova, E.V., Krivonogov, S.K., 2009. Late Glacial and Holocene changes  
749 in vegetation cover and climate in southern Siberia derived from a 15 kyr long pollen  
750 record from Lake Kotokel. *Climate of the Past* 5, 285-295.
- 751 ter Braak, C.J.F., Šmilauer, P., 2002. CANOCO reference manual and user's guide to  
752 CANOCO for Windows: Software for Canonical Community Ordination version 4.5.  
753 Microcomputer Power, Ithaca, New York.
- 754 Thompson, R., Oldfield, F., 1986. *Environmental Magnetism*. George Allen and Unwin,  
755 London, 227 pp.
- 756 Wang, Y., Cheng, H., Edwards, R.L., He, Y., Kong, X., An, Z., Wu, J., Kelly, M.J., Dykoski,  
757 C.A., Li, X., 2005. The Holocene Asian monsoon: links to solar changes and North  
758 Atlantic climate. *Science* 308, 854-857.
- 759 Weber, A.W., Link, D.W., Katzenberg, M.A., 2002. Hunter-gather culture change and  
760 continuity in the middle Holocene of the cis-Baikal, Siberia. *Journal of  
761 Anthropological Archaeology* 21, 230-299.
- 762 Weber, A.W., Katzenberg, M.A., Schurr, T.G., (Eds.), 2010. *Prehistoric Hunter-Gatherers of  
763 the Baikal Region, Siberia: Bioarchaeological Studies of Past Lifeways*. University of  
764 Pennsylvania Press, Philadelphia, USA.
- 765 White D., Bush A.B.G., 2010. Holocene climate, environmental variability and Neolithic  
766 biocultural discontinuity in the Lake Baikal region. In *Prehistoric Hunter-Gatherers of  
767 the Baikal Region, Siberia: Bioarchaeological Studies of Past Lifeways*, Weber AW,  
768 Katzenberg MA, Schurr TG (eds) Pennsylvania; University of Pennsylvania Museum  
769 Press: 1-26
- 770 Wünneman, B., Demske, D., Tarasov, P., Kotlia, B.S., Reinhardt, C., Bloemendal, J.,  
771 Diekmann, B., Hartmann, K., Krois, J., Riedal, F. Arya, N., 2010. Hydrological  
772 evolution during the last 15 kyr in the Tso Kar lake basin (Ladakh, India), derived  
773 from geomorphological, sedimentological and palynological records. *Quaternary  
774 Science Reviews* 29, 1138-1155.



775 Zhao, Y., Yu, Z., Chen, F., Ito, E., Zhao, C., 2007. Holocene vegetation and climate history at  
776 Hurleg Lake in the Qaidam Basin, northwest China. *Review of Palaeobotany and*  
777 *Palynology* 145, 275-288  
778  
779

780  
781  
782  
783  
784  
785  
786  
787  
788  
789  
790  
791  
792  
793  
794  
795  
796  
797  
798  
799  
800  
801  
802  
803  
804  
805  
806  
807  
808  
809  
810  
811  
812  
813  
814  
815  
816  
817  
818  
819  
820  
821  
822  
823

## Figure Legends

Fig. 1. Map of Lake Baikal and its immediate catchment, showing the location of key sites: Lake Khall, Ol'khon region, Lake Kotokel and Primorsky Mountain Range.

Fig. 2. Age-depth model based on  $^{137}\text{Cs}$  and calibrated radiocarbon AMS dates, constructed using 'Bacon' (Blaauw and Christen, 2011). Grey-shaded area represents 95% confidence intervals of modelled ages (black line).

Fig. 3. Pollen, spore and *Pediastrum* coenobia colony relative abundances plotted on the calibrated age scale. Taiga biome scores are also shown – see section 3.2 for details. Significant PCA axis 1 sample scores (+ eigenvalue; EV) and significant compositional turnover (beta diversity; SD units) value for vegetation data is also given ( $p = 0.05$ ;  $n=499$ ). Pollen zones have been delimited using optimal partitioning.

Fig. 4. Total ostracod concentrations (valves/g) are plotted on the calibrated age scale, along with the two most abundant genera *Lymnocythere* sp. and *Candona* sp. The concentration of blackened valves is also given.

Fig. 5. Low-frequency magnetic susceptibility measurements and particle size statistics produced from Folk and Ward (1957) method (mean particle size, sorting, skewness and kurtosis). Sedimentary mean values are shown with a vertical line for each of mean particle size, sorting, skewness and kurtosis.

Fig. 6. PCA biplot of geochemical data. Axis 1 is plotted against axis 2. Axis 1 accounts for significant 73.8% variation in element data. Axis 2 accounts for only 10.0% variation in the data which broken stick shows is not significant.

Fig. 7. Geochemical stratigraphy of Lake Khall. Selected major elements are shown, expressed either as percentages (Al, Ti, K, Si, P, S, Mn, Fe) or concentrations ( $\mu\text{g/g}$ : Rb, Pb, Ca, Sr). Significant PCA axis 1 sample scores (+ eigenvalue; EV) are also shown.

Fig. 8. Composite stratigraphical plot showing: (i) pollen DCCA axis 1 sample scores; (ii) mean grain size; (iii) pollen-inferred reconstruction anomalies (total annual precipitation – Pann; mean temperature of the coldest month – Tc; mean temperature of the warmest month – Tw); (iv) geochemical ratio of selected elements Sr/Ca ( $\times 1000$ ), Ca/Al, P/Al, Ti/K, K/Rb; (v) concentrations of *Candona* sp.; (vi) oxygen isotope data from Lake Baikal biogenic silica (Mackay et al., 2011); (vii) oxygen isotope data from Dongge Cave, southern China (Wang et al., 2005); (viii) palaeo-temperatures inferred from the GRIP borehole ( $^{\circ}\text{C}$ ) (Dahl-Jensen et al., 1998); (ix) July insolation at  $60^{\circ}\text{N}$  ( $\text{W/m}^2$ ) (Berger and Loutre, 1991)

Figure 1

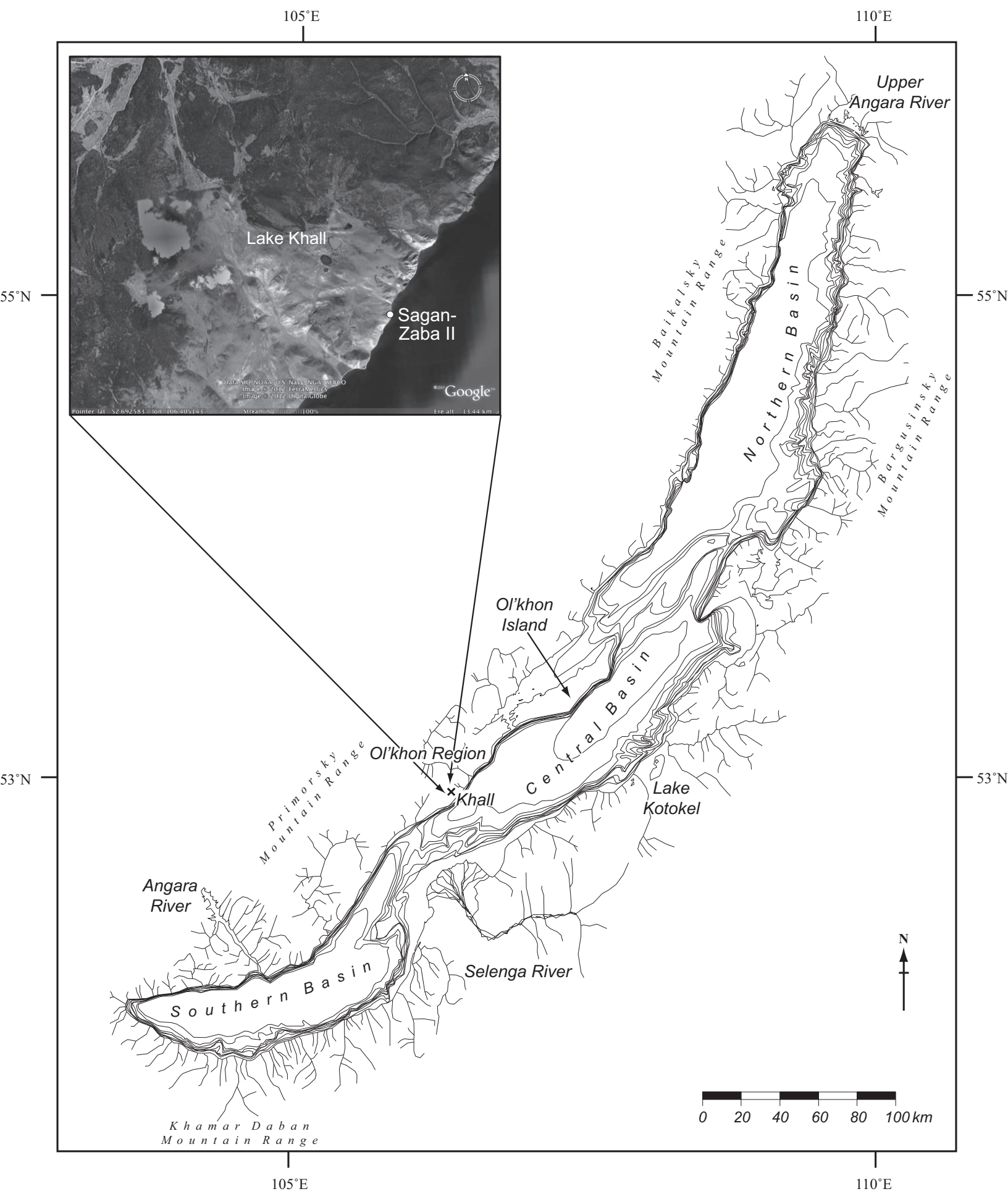


Figure 2

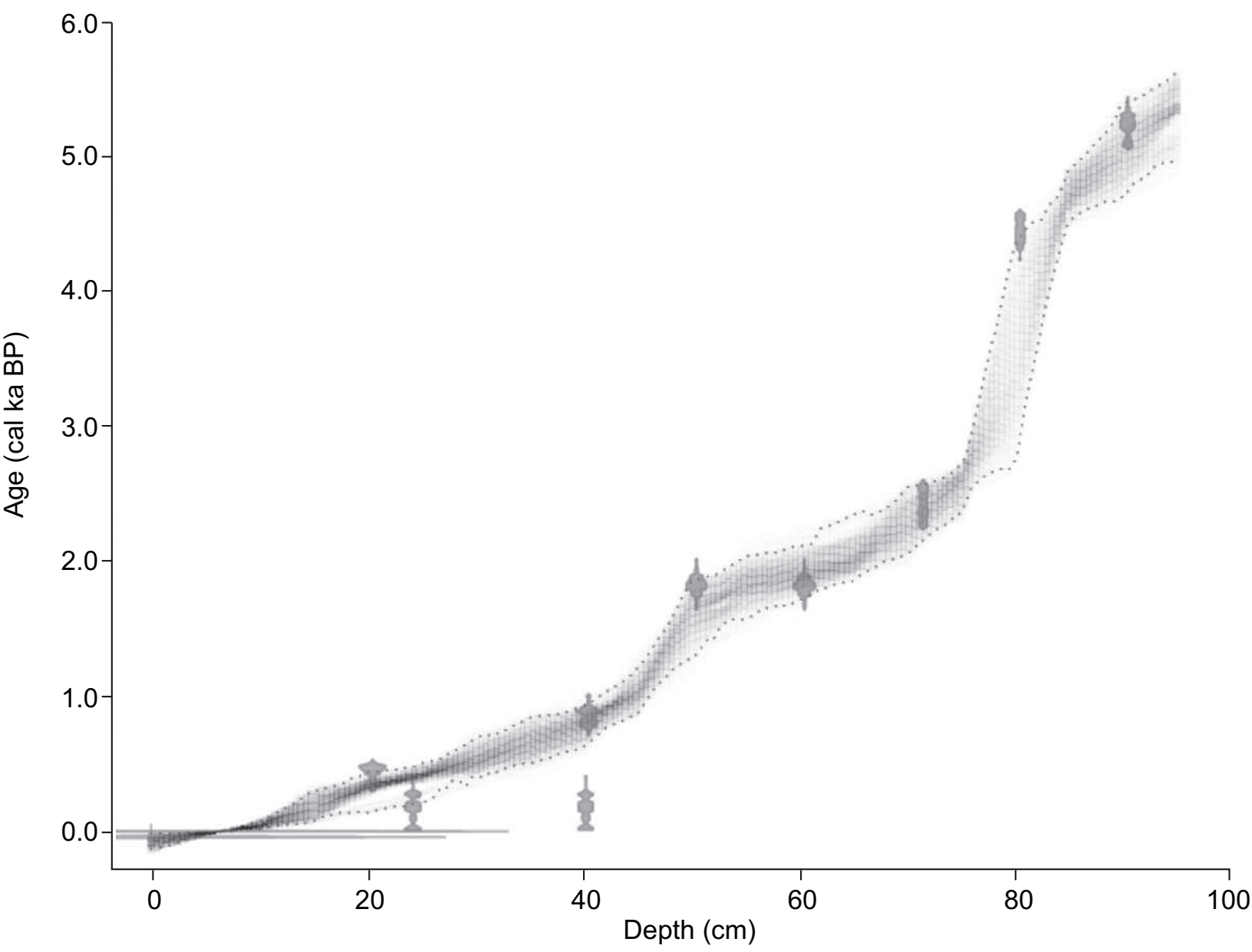


Figure 3

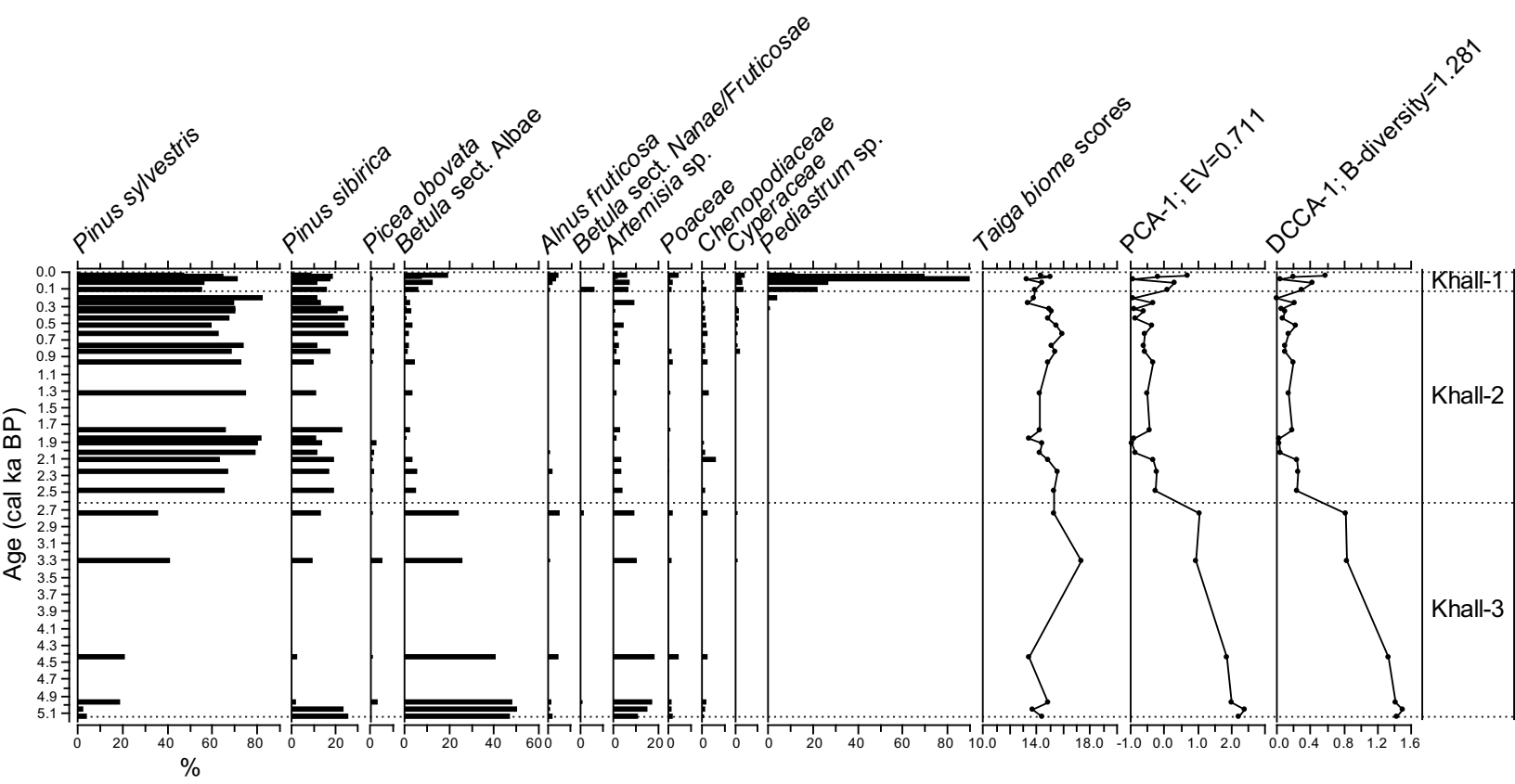


Figure 4

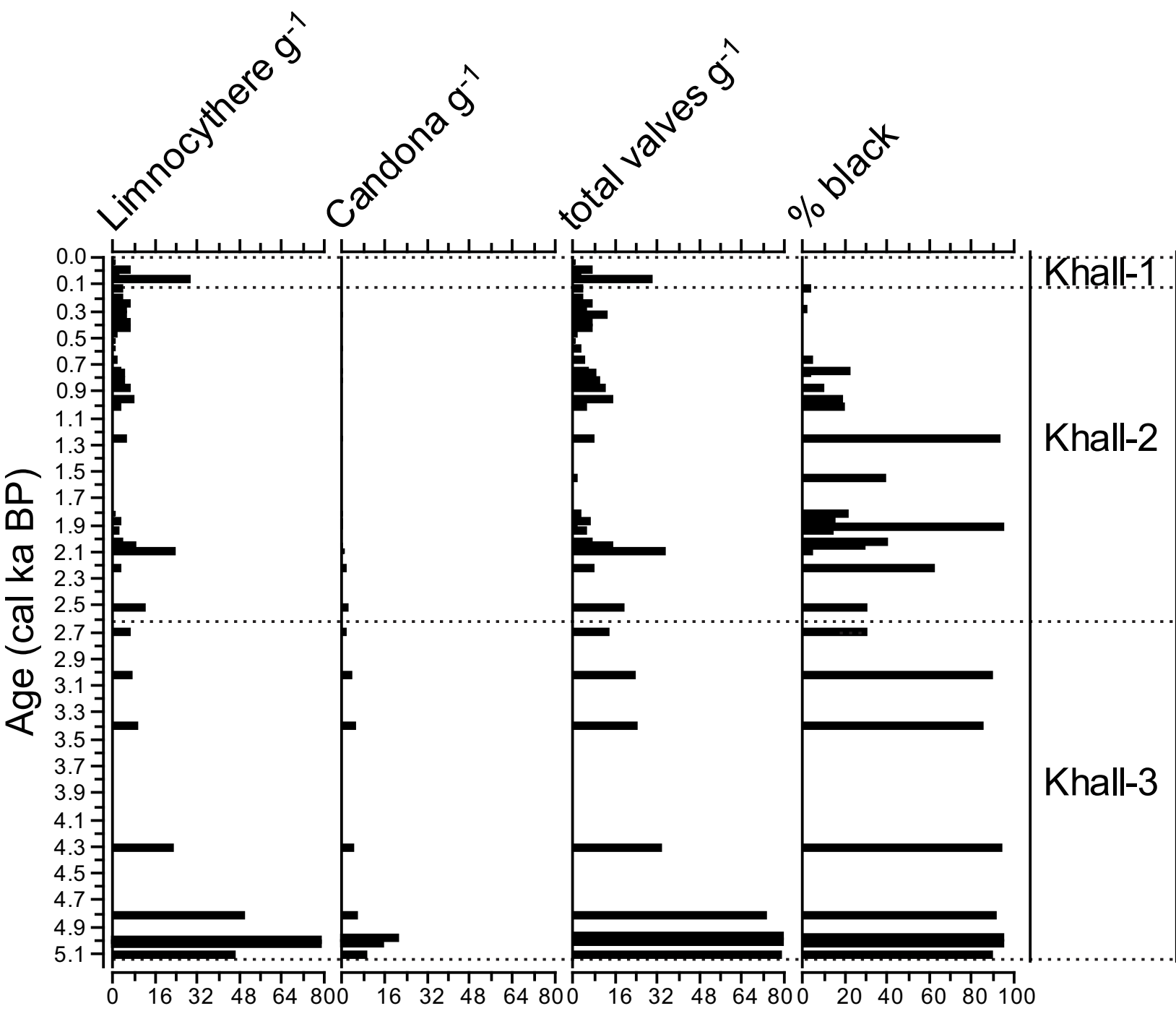


Figure 5

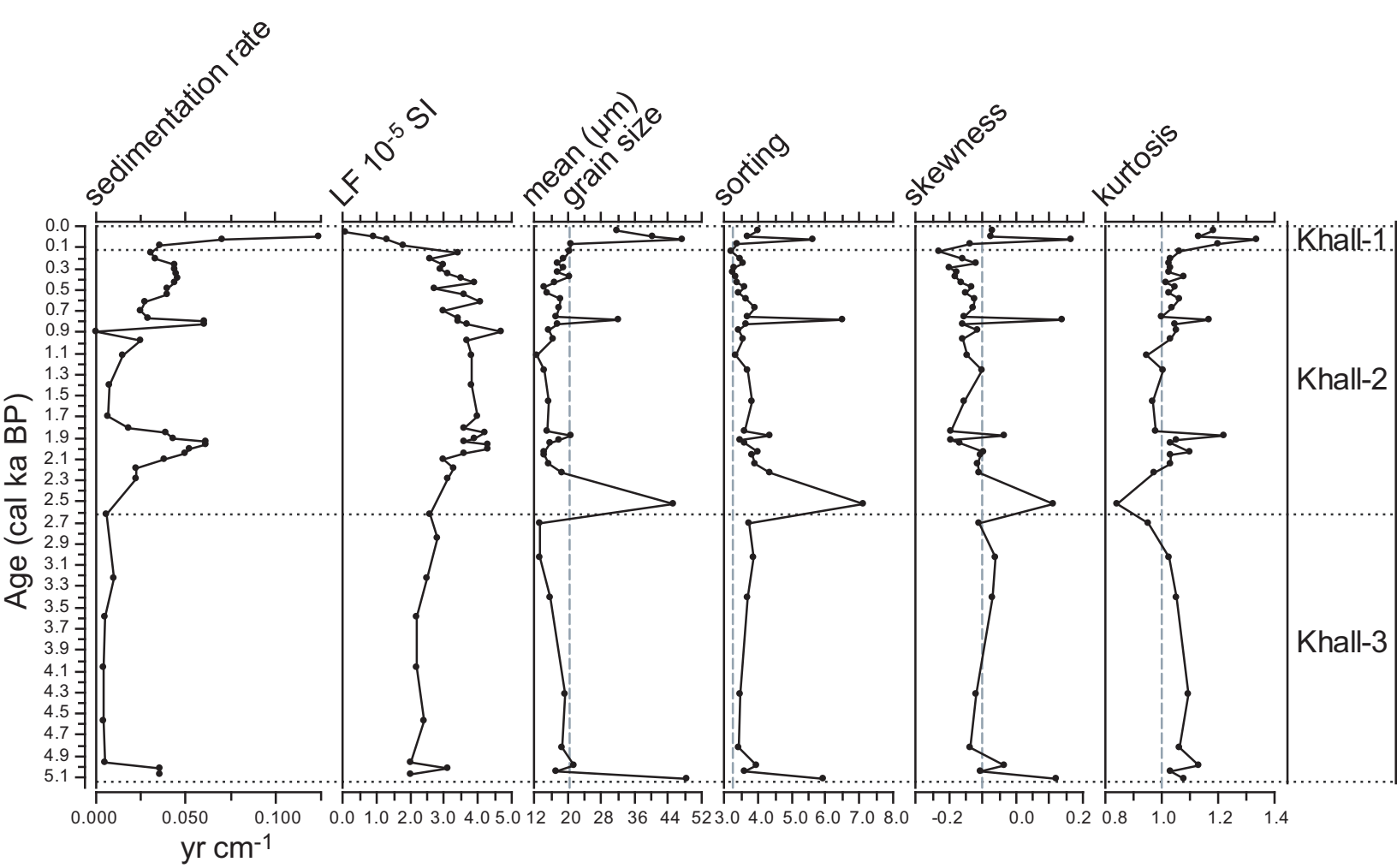


Figure 6

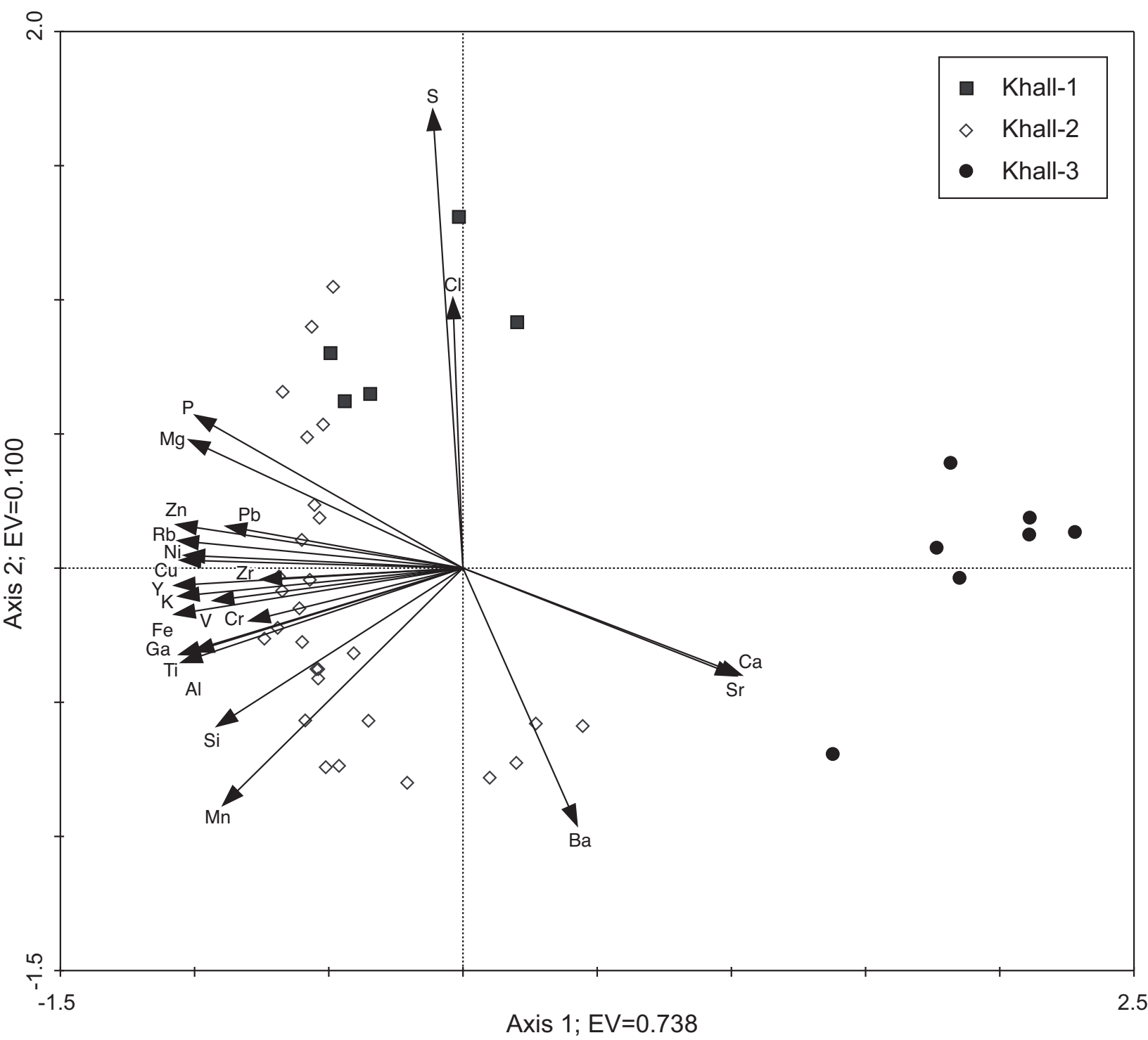




Figure 7

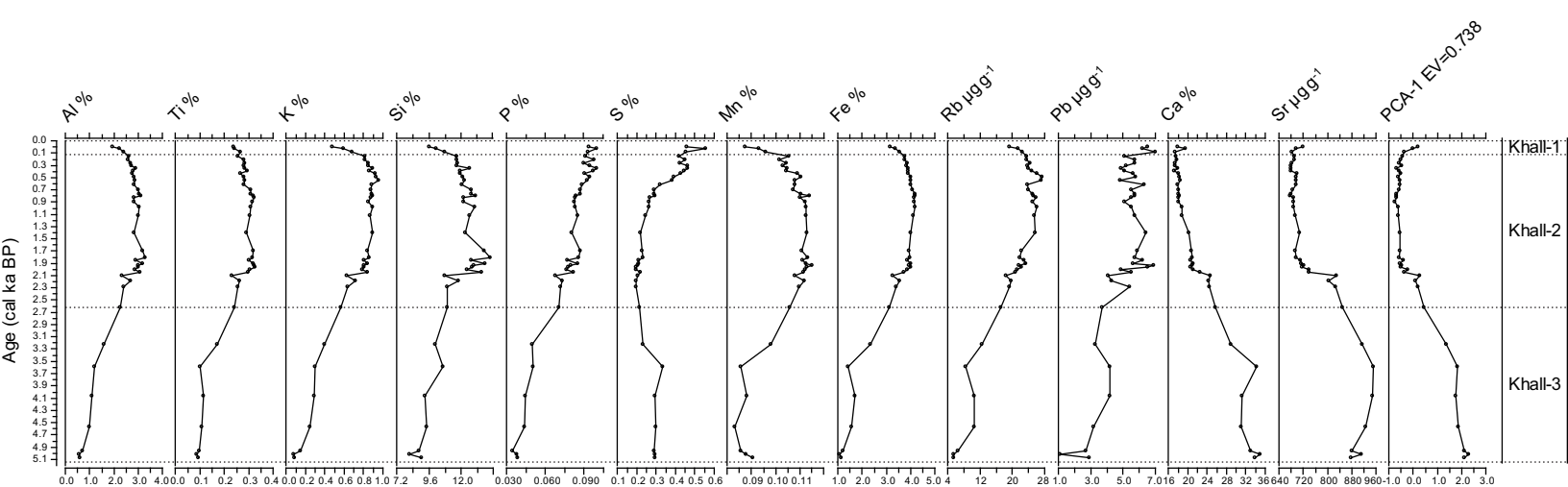


Figure 8

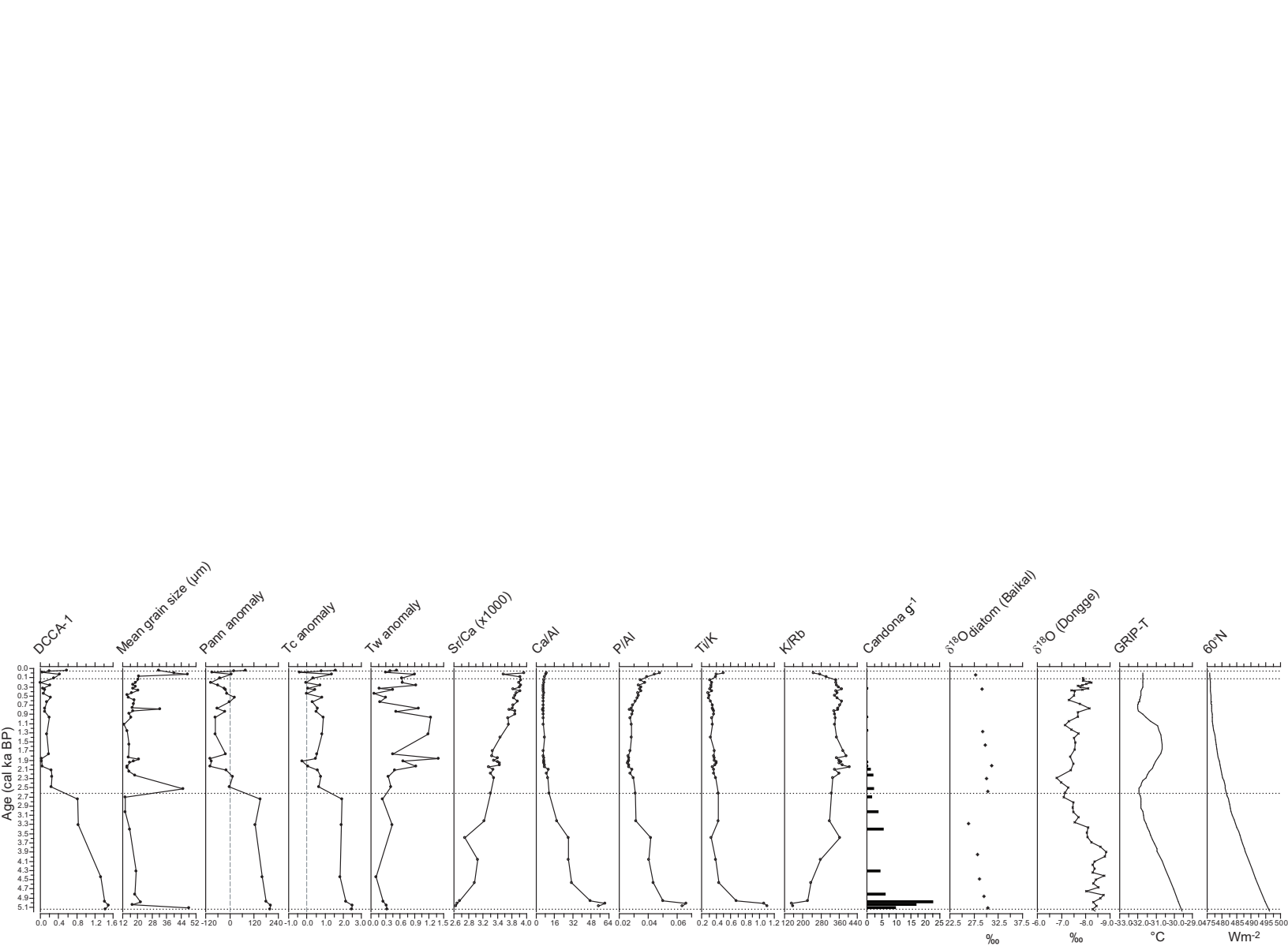


Table 1: Results of AMS radiocarbon dating for Lake Khall sediment core. Depth range and mid-depth are the original depths of samples from core. Calibration of independent  $^{14}\text{C}$  dates from the core was performed using IntCal09 radiocarbon calibration curve (Reimer et al., 2009) and OxCal software ver. 4.1.7 (Bronk Ramsey, 2009), assuming the reservoir correction of  $150\pm 50$  years.

Sample code	Sample material	Depth range, cm	Mid-depth, cm	$^{14}\text{C}$ age BP	Calibrated age range calBP (68.2%)		Calibrated age range calBP (95.4%)	
Poz-25686	Contemporary macrophytes	n/a	n/a	105.58 $\pm$ 0.33 pMC	n/a	n/a	n/a	n/a
Poz-30449	TOC	20-21	20.5	555 $\pm$ 30	626	532	640	519
Poz-25740	<i>Potamogeton</i> seed	24-24.5	24.25	345 $\pm$ 30	465	319	485	313
Poz-25682	<i>Potamogeton</i> seed	40-40.5	40.25	330 $\pm$ 30	455	316	474	308
Poz-30448	TOC	40-41	40.5	1140 $\pm$ 30	1072	980	1169	968
Poz-33695	TOC	50-51	50.5	2110 $\pm$ 35	2131	2009	2295	1992
Poz-30447	TOC	60-61	60.5	2105 $\pm$ 30	2123	2010	2150	1995
Poz-33696	TOC	71-72	71.5	2605 $\pm$ 35	2759	2724	2787	2545
Poz-25683	<i>Potamogeton</i> seed	80-81	80.5	4285 $\pm$ 35	4865	4835	4964	4822
Poz-25684	<i>Potamogeton</i> seed	90-91B	90.5	4930 $\pm$ 70	5730	5596	5892	5487